[CANCER RESEARCH 64, 5779–5786, August 15, 2004]

Suppression of Human Prostate Tumor Growth in Mice by a Cytolytic D-, L-Amino Acid Peptide: Membrane Lysis, Increased Necrosis, and Inhibition of Prostate-Specific Antigen Secretion

Niv Papo,[1] Amir Braunstein,[1] Zelig Eshhar,[2] and Yechiel Shai[1]

Departments of [1]Biological Chemistry and [2]Immunology, The Weizmann Institute of Science, Rehovot, Israel

ABSTRACT

Gene-encoded host defense peptides are used as part of the innate immunity, and many of them act by directly lysing the cell membrane of the pathogen. A few of these peptides showed anticancer activity *in vitro* but could not be used *in vivo* because of their inactivation by serum. We designed a 15-amino acid peptide, composed of D- and L-amino acids (diastereomer), which targets both androgen-independent and androgen-dependent human prostate carcinoma cell lines (CL1, 22RV1, and LNCaP). Most importantly, we observed a complete arrest of growth in CL1 and 22RV1 xenografts treated intratumorally with the diastereomer. This was also accompanied by a lowering of prostate-specific antigen serum levels secreted by the 22RV1 xenograft. Furthermore, the diastereomer synergized with conventional chemotherapeutics. In contrast, the parental all L-amino acids peptide was highly active only *in vitro* and could not discriminate between tumor and nontumor cells. Fluorescent confocal microscopy, histopathologic examination, and cell permeability studies (depolarization of transmembrane potential and release of an encapsulated dye) suggest a necrotic mechanism of killing, after a threshold concentration of peptide has been reached. Its destructive killing effect and the simple sequence of the diastereomer make it an attractive chemotherapeutic candidate possessing a new mode of action, with potential to be developed additionally for the treatment of prostate carcinoma.

INTRODUCTION

Prostate carcinoma is considered the most common nonskin cancer in America. It accounts for ~30% of all of the major cancers in men, which is more than twice the next most common cancer (1–3). Prostate carcinoma is also the cancer with the largest expected increase in the next decade, with a projected annual incidence rising to 300,000 cases and an annual death rates reaching 50,000 by the year 2015 (reported by the Prostate Cancer Foundation). The approaches used currently to combat prostate carcinoma are surgery, irradiation, or chemotherapic (4–6). Chemotherapeutic drugs damage cancer cells by a variety of mechanisms (*e.g.*, DNA cleavage/alkylation and topoisomerase II inhibition) that are eventually translated into apoptotic signals. Unfortunately, prostate carcinoma, in contrast to several other cancers, does not respond well to single or multiple drug regimens, especially in the case of androgen-independent cancer (7–10). In addition, chemical anticancer agents are nonspecific and, consequently, damage healthy tissues as well. This has stimulated the search for new drugs with new modes of action and with a potential to overcome the inherent resistance. Examples include the development of polypeptides that control apoptosis (11–13), or alternatively, peptides that lyse cells. Indeed, cell lytic antimicrobial peptides have been shown to act *in vitro* against different types of cancer cells (14–17). These peptides have a central role in the innate immunity of all of the organisms, including insects, amphibians, and mammals (18). Examples include human defensins (19–21), cecropins (22), cecropin-magainin hybrids (23, 24), magainins (14), peptides conjugated to homing domains (15–17), propeptides (25), and others (26, 27). These peptides preferentially bind and disrupt negatively charged phospholipid membranes, the major component of the bacterial cytoplasmic membrane. However, it is not clear why some of them bind better and kill cancer cells compared with normal cells (28, 29).

Despite the potent anticancer activity of these peptides *in vitro*, studies *in vivo* are very limited, mainly because of their inactivation in serum, partially because of their binding to serum components and their enzymatic degradation. Examples include the following data: (*a*) apoptotic peptides targeted to specific tissues by conjugating them to homing domains (15, 16); and (*b*) i.p.-injected antimicrobial peptides derived from magainin and its all D-amino acid analog against ovarian cancer (14).

We have shown recently that incorporation of D-amino acids into noncell-selective lytic peptides made them selective toward bacteria (30). Some of these peptides were also lytic to cancer cells (29). Most importantly, this family of peptides preserved their activity in serum, and their enzymatic degradation could be controlled. One peptide, a 15-amino acids diastereomer composed of leucines, arginines, and lysines, was shown recently to act against the mouse melanoma and lung carcinoma cell lines and to significantly inhibit lung metastasis in mice with no detectable side effects (31). Here, we show that a 15-mer all L-amino acids lytic peptide and its diastereomer, both of which are composed of only lysines and leucines, are highly active preferentially toward both androgen-dependent and androgen-independent human prostate carcinoma cells. Most importantly, the diastereomer, but not its all-L amino acids parental peptide, completely inhibited the growth of several human prostate tumor xenografts and markedly reduced the secretion of the prostate-specific antigen (PSA) produced by the 22RV1 xenografts. In contrast, a 12-amino acids diastereomer and two other native antimicrobial peptides, with antimicrobial activity similar to that of the 15-amino acids diastereomer, were either inactive or nonselectively active toward cancer cells compared with noncancer cells. The 15-amino acids diastereomer was additionally evaluated for its ability to act synergistically with other chemotherapeutic agents and for its plausible mode of action, by using confocal fluorescence microscopy, fluorescently labeled peptide, and cell-permeable markers. The results are discussed with respect to a necrotic-like mode of action for the diastereomer and its advantages over all L-amino acids lytic peptides for future development as a new chemotherapeutic agent with a new mode of action.

MATERIALS AND METHODS

Cell Culture

The CL1 human prostate carcinoma cell line is an androgen-independent subclone of LNCaP, which was generated by culturing androgen-dependent LNCaP cells in charcoal-stripped, androgen-de-

Received 4/23/04; revised 6/8/04; accepted 6/15/04.

Grant support: The Association of the Cure of the Cancer of Prostate, the Israel Cancer Association, and The Harold S. and Harriet B. Brady Professorial Chair in Cancer Research (Y. Shai).

The costs of publication of this article were defrayed in part by the payment of page charges. This article must therefore be hereby marked *advertisement* in accordance with 18 U.S.C. Section 1734 solely to indicate this fact.

Note: N. Papo and A. Braunstein contributed equally to this study.

Requests for reprints: Yechiel Shai, the Department of Biological Chemistry, The Weizmann Institute of Science, Rehovot, 76100 Israel. Phone: 972-8-9342711; Fax: 972-8-9344112; E-mail: Yechiel.Shai@weizmann.ac.il.

pendent serum as described previously (32). The 22RV1 human prostate carcinoma cells are androgen-independent subclones of the androgen-dependent prostatic adenocarcinoma CWR22 xenograft (33). CL1 and 22RV1 (American Type Culture Collection, Manassas, VA) were grown in RPMI 1640 supplemented with 10% FCS (Biological Industries, Beit Haemek, Israel). Androgen-dependent LNCaP human prostate carcinoma cells (34) were grown similarly to CL1 but with the addition of 5 μg/ml insulin and 10 nM testosterone (Sigma Chemical Co.). NIH-3T3 mouse fibroblast cell lines (American Type Culture Collection) were grown in DMEM supplemented with 10% BSA. OL human foreskin fibroblasts (American Type Culture Collection; a generous gift from Professor Menachem Rubinstein, Weizmann Institute of Science, Rehovot, Israel) were maintained in 10% FCS and 90% DMEM.

Peptide Synthesis, Rhodamine Labeling, and Purification

Peptides were synthesized by a F-moc solid-phase method on Rink amide 4-methyl benzhydrylamine resin (Calibochem-Novabiochem, La Jolla, CA; Ref. 35), using a ABI 433A automatic peptide synthesizer, and purified as described previously in detail (31). Labeling of the NH_2 terminus of the peptides with rhodamine was done on the resin-bound peptide (36). The purified peptides were shown to be homogeneous (>99%) by analytical high-performance liquid chromatography. Finally, the peptides were subjected to amino acid analysis and electrospray mass spectroscopy to confirm their composition and molecular weights.

In Vitro Cytotoxicity Assays

Aliquots of medium containing 1×10^4 cells were distributed into a 96-well plate (Falcon). The following day, the media were replaced with 90 μl of fresh media and 10 μl of a solution containing different concentrations of the peptides. The plate was then incubated for 24 h before adding to each well 50 μl of 2,3-bis[2-methoxy-4-nitro-5-sulfophenyl]-2*H*-tetrazolium-5-carboxanilide inner salt (XTT) reaction solution (Biological Industries); viability was determined as described previously (31). The LC_{50} (concentration at which 50% of the cells die) for each peptide was obtained from the dose-dependent cell viability curves. The kinetics of cell killing was also monitored by using the LC_{100} (concentration at which 100% of the cells die) of the peptide (50 μM, 80 μM, 300 μM, and 400 μM, for CL1, 22RV1, OL, and 3T3 cells, respectively).

The toxicity of the peptides against human red blood cells (4% v/v) was also investigated as described previously (30). Controls for zero hemolysis (blank) and 100% hemolysis consisted of human red blood cells suspended in PBS and 1% Triton (Sigma), respectively.

Detection of Cell Permeability Induced by the Peptide

Depolarization of Transmembrane Potential. Cells were incubated with 1 μM diS-C_3-5 (Molecular Probes, Eugene, OR), and the fluorescence intensity was recorded until a plateau was reached (λex = 620 nm; λem = 670 nm). The peptide (final concentration of 0.1–100 μM), dissolved in PBS, was then added to 50 μl of the fluorescently labeled cells to make a final volume of 100 μl (the number of cells/well was similar to those in the XTT viability assay). The resulting suspension was incubated with agitation for 60 min at 37°C. Membrane depolarization was monitored by observing the change in the intensity of fluorescence emission of the membrane-potential-sensitive dye. The control for zero membrane depolarization (blank) consisted of fluorescently labeled cells suspended in PBS. One hundred percent membrane depolarization was set as the difference in fluorescence intensity between zero and 60 min after adding the dye to the cells.

Calcein Leakage from Cells

Calcein fluorophore (Hach Chemical Co., Loveland, CO; 1 μM, a self-quenching concentration) was entrapped into the above cells by incubation for 1 h (0.4×10^6 cells/ml in 10 ml of PBS). The nonencapsulated calcein was removed from the cells by centrifugation. Cells were resuspended in PBS, and the peptide (final concentration 0.1–100 μM) was added to the cell suspensions. Peptide-induced calcein leakage resulted in an increase of fluorescence (37); it was monitored at room temperature (λex = 485 nm; λem = 515 nm). Complete dye release (100% activity) was obtained after disrupting the cells with Triton X-100 (0.1% final concentration). Under the experimental conditions, in the absence of peptide, the leakage rate was <1% in 5 h. The kinetics of transmembrane potential depolarization and calcein leakage was also monitored. For this assay we used the LC_{100} of the peptide (50 μM, 80 μM, 300 μM, and 400 μM, for CL1, 22RV1, OL, and 3T3 cells, respectively).

Confocal Fluorescence Microscopy Studies

Confocal images were obtained using an Olympus IX70 FV500 confocal laser scanning microscope. Briefly, cells were placed on a coverslip, and a series of images were taken before and 3 min after the addition of rhodamine-labeled peptide (5 μM in PBS), using oil immersion. The kinetics of peptide binding and cell lysis was also followed using the rhodamine-labeled peptide at its LC_{100} for each cell. The setting of the photomultipliers (gain and black level) was constant for the series of images. Care was taken so that any existing photobleaching did not compromise the interpretation and laser irradiation, and other means of illumination were prevented between images. The confocal images were obtained at a 12-bit resolution.

Measurements of Synergism by Using Checkerboard Titrations

Synergistic activities were assayed by checkerboard titrations with RPMI 1640. Fractional lethal concentration (FLC) indices were calculated by using the following formula:

$$[(A)/LC_{100A}] + [(B)/LC_{100B}] = FLC_A + FLC_B = \text{FLC index},$$

where LC_{100A} and LC_{100B} are the LC_{100}s of drugs A and B when used alone, and (A) and (B) are the LC_{100}s of drugs A and B when used in combination. Drug A stands for the peptide, and drug B stands for doxorubicin or cyclophosphamide (Sigma); the cells used were CL1, 22RV1, and LNCaP human prostate carcinoma cells (grown and treated as described previously). The interaction between the peptide and the chemotherapeutic agent was defined as synergistic if the FLC index was 0.5 or less, additive if the FLC index was >0.5–1.0, indifferent if the FLC index was >1.0–2.0, and antagonistic if the FLC index was >2.0 (38).

Studies with Prostate Carcinoma Xenografts

Inhibition of Tumor Growth in Human Prostate Carcinoma Xenografts. The s.c. implantation of human prostate carcinoma in mice was done as described previously (39). Briefly, 0.1 ml of androgen-independent CL1 and 22RV1 human prostate carcinoma cells (5×10^6 cells) in Matrigel (Biological Industries) was inoculated s.c. into the dorsal side of 5–6-week-old nude male mice weighing 20–25 g (Harlen Co., Jerusalem, Israel). Two weeks after cell implantation, when the tumor diameter reached ≥5 mm (we denoted this day as day 1), the all L-amino acids peptide and its diastereomer (at 1 mg/kg; 0.1 mM) or vehicle (PBS; pH = 7.4) were injected intratumorally (dosing volume of 2.5 ml/kg) three times a week for a total of 9 doses. Tumor size was measured by a caliper and recorded twice a week during a period of 28 days. Mice were weighed, and tumor weight (mg) was estimated by using the formula of length × width × depth × 0.52 in mm^3, assuming the specific gravity to be 1. At the end of the treatment, the mice were killed, and the

tumors were removed, photographed, and weighed. The animal experimentation was reviewed and approved by the Institutional Animal Care and Use Committee.

Serum PSA Levels

Four weeks after the first treatment, blood was withdrawn from the 22RV1-inoculated mice to determine the level of PSA. The blood samples were taken directly to heparin-containing tubes, centrifuged, and the supernatants were stored at −20°C. The CanAg PSA EIA kit (CanAg Diagnostics) was used to determine the total PSA in the mice plasma (39). Tumor weight and PSA levels, represented as the mean ± SE, were calculated from the raw data and then subjected to Student's *t* test. A value of $P < 0.05$ was considered as statistically significant.

RESULTS

We synthesized an amphipathic all L-amino acids peptide and its diastereomer, designated as amphipathic-L (LKLLKKLLKKLLKLL-NH_2), and amphipathic-D (LK*L*LK*K*L*LK*KLL*K*LL-NH_2, underlined and italic letters are D-amino acids). The data presented below demonstrated that only amphipathic-D could arrest the growth of human prostate carcinoma xenografts, and, therefore, most experiments regarding mode of action were performed only with this peptide.

***In Vitro* Activity of the Peptides toward Androgen-Dependent and Androgen-Independent Human Prostate Carcinoma Cells.** The activity of amphipathic-L and -D was tested against various cell lines. We used as controls a 12-mer diastereomer (KL*LL*KLK*L*K*L*LK-NH_2, underlined and italic letters are D-amino acids), the bee venom melittin and its diastereomer (melittin-D; Ref. 30, 40), and the human cathelicidin LL-37 (41), all of which have potent antimicrobial activity. The chemotherapeutics doxorubicin and mitomycin C (Sigma Chemical Co.) were used as additional controls. The LC_{50}s of the peptides are shown in Table 1. The data reveal that amphipathic-D is the most selective peptide toward prostate carcinoma cells. In addition, amphipathic-D is not hemolytic toward human erythrocytes at the maximal concentration tested, whereas amphipathic-L, LL-37, and melittin are highly hemolytic (Table 1). Note that the kinetics of cell killing using LC_{100} values (shown in Fig. 1*A*, right panel) is very rapid and is similar in all cell types.

Depolarization of Transmembrane Potential and the Release of Entrapped Calcein from Cells Induced by Amphipathic-D. Amphipathic-D induced depolarization of transmembrane potential (Fig. 1*B*) and leakage of entrapped calcein (Fig. 1*C*) from cells. Importantly, the data revealed a direct correlation between the LC_{50} values of the peptide toward all of the cells (Table 1; Fig. 1*A*, left panel) and the dose-dependent potential depolarization (Fig. 1*B*, left panel) and calcein leakage (Fig. 1*C*, left panel). This suggests that the cell membrane is one of the targets. As expected, the peptide could not dissipate the transmembrane potential of erythrocytes, in agreement with its nonhemolytic activity (data not shown).

We also followed the kinetics of membrane depolarization (Fig. 1*B*, right panel) and calcein release (Fig. 1*C*, right panel) as a function of time at the LC_{100} of the peptide. The data revealed that the kinetics of cell killing (Fig. 1*A*, right panel) is similar to the kinetics of the two membrane disruption assays. These results additionally suggest that membrane disruption is the lethal event for all of the cells tested.

The Addition of Amphipathic-D Triggers Necrosis of Prostate Carcinoma Cells. Amphipathic-D was labeled with rhodamine at its NH_2 terminus (without affecting its anticancer activity) and then incubated (5 μM peptide) with the cells. The cells were then washed and observed for residual rhodamine. The data revealed that the peptide bound strongly and preferentially to the CL1 (Fig. 2*A*, lower panel) and 22RV1 (Fig. 2*B*, lower panel) prostate carcinoma cells and significantly less to OL foreskin fibroblasts (Fig. 2*C*, lower panel). The peptide was additionally incubated with the cells at its LC_{100} values, and images were taken. Fig. 2*D* shows examples of images of CL1 cells after treatment for 2, 3, and 5 min with 50 μM of the rhodamine-labeled amphipathic-D. The cells died as a result of acute injury, swelling (after 3 min), and bursting (after 5 min), leaving only the nucleus intact. This suggests a necrotic mode of action.

The kinetics of binding of the peptide (at its LC_{100} value) to cells was also monitored. The data reveal >80% binding to all of the cells already after ~3 min and complete binding after ~5 min. Note that ~80% of membrane leakage (depolarization of *trans*-membrane potential and calcein release experiments) took place a few minutes after the binding of the peptide (Fig. 1, *B* and *C*, right panels).

Synergistic Effect between Amphipathic-D and Doxorubicin against Androgen-Dependent and Androgen-Independent Prostate Carcinoma Cells. Checkerboard titrations were performed using amphipathic-D in combination with doxorubicin and cyclophosphamide against the CL1, 22RV1, and LNCaP cell lines (Table 2). The LC_{100} values of doxorubicin against CL1 and LNCaP cells was found to be 200 μM and 30 μM, respectively, and the LC_{100} values for cyclophosphamide against CL1, 22RV1, and LNCaP cells were 1000 μM, 3000 μM, and 5000 μM, respectively. The peptide was incubated for 2 min with the cells before adding the drugs. The peptide showed a significant synergism with doxorubicin against the three cell lines (FLC < 0.5). For example, the FLC value of 0.44 (Table 1) corresponds to a combination of .25 and .20 of the LC_{100} values of amphipathic-D and doxorubicin, respectively. In contrast, only an additive effect was found when the peptide was combined with cyclophosphamide (0.5 < FLC < 1.0). The results were similar when the peptide was incubated for 60 min before adding the drugs or when the order of the addition was reversed. Note that in all of the cases,

Table 1 *Lethal concentrations (LC_{50} in μM)* of the peptides detected by XTT assay*

Peptide designation	Nonmalignant cells		Human prostate carcinomas			% Hemolytic activity at 100 μM
	NIH-3T3 mouse fibroblasts	OL foreskin fibroblasts	CL1 prostate carcinoma	22RV1 prostate carcinoma	LNCaP prostate carcinoma	
12-mer	>100	50	100	>50	>50	0
Amphipathic-D	100	35	3	6	5	0
Amphipathic-L	7	5	4	4	6	100
LL-37	28	14	6	12	8	25
Melittin	10	3	2	2	4	100
Melittin-D	>50	>50	>50	>50	>50	0
Doxorubicin†	ND	ND	120	ND	9	0
Mitomycin C	3	2	5	6	8	0

Abbreviation: ND, not determined.

* Results are the mean of three independent experiments each performed in duplicate, with SD not exceeding 10%. Amphipathic-D is similarly potent against other cancer cell lines (29).

† LC_{50} values for doxorubicin were taken from An *et al.* (51) and repeated in this study.

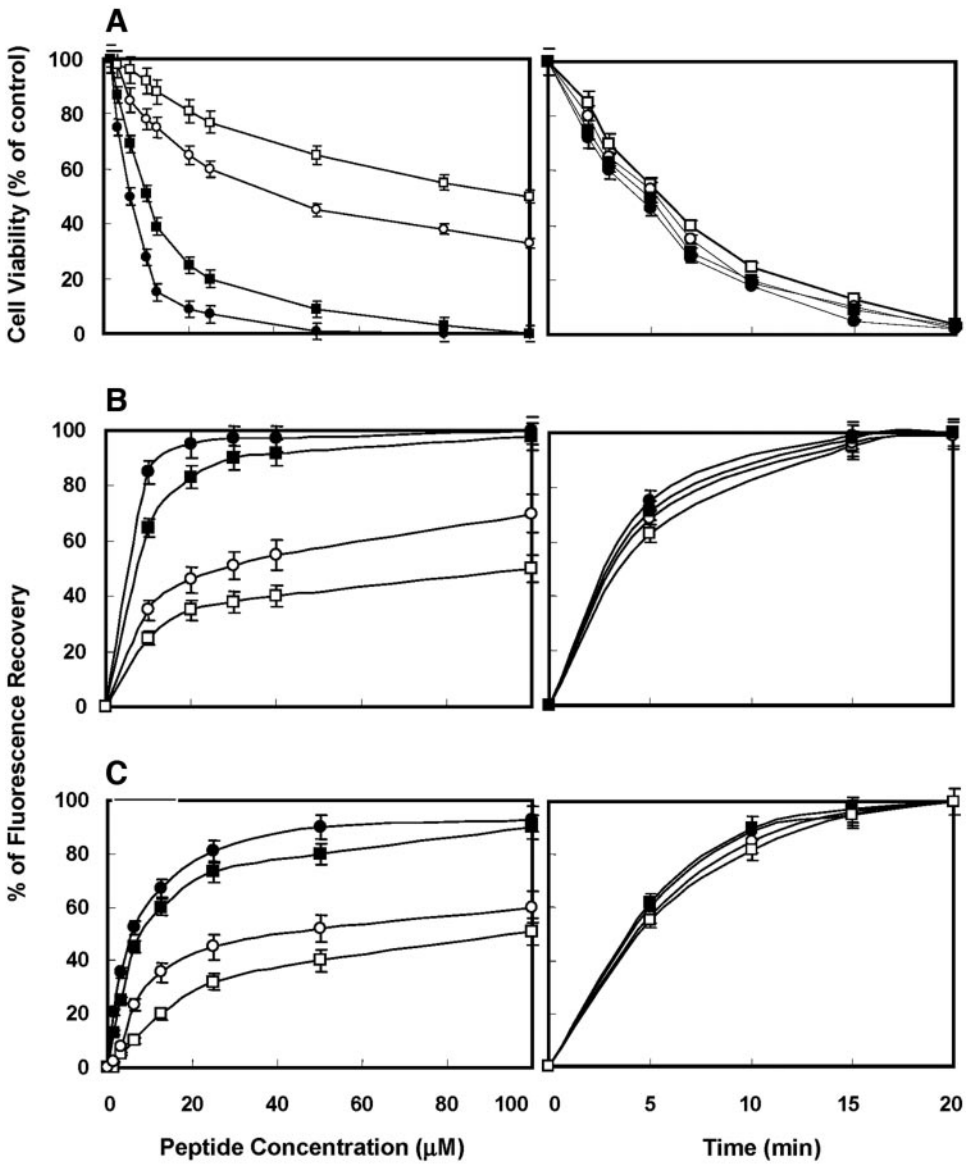

Fig. 1. *A*, dose-dependent (*left panel*) and time-dependent (*right panel*) effects of amphipathic-D in growth inhibition of the different cell lines. Amphipathic-D was incubated for 24 h with the cells before adding XTT. Cell viability was determined relative to the control. *B*, maximal dissipation of the membrane potential as a function of amphipathic-D concentration (*left panel*) and time (*right panel*). Membrane depolarization was monitored by observing the change in the intensity of fluorescence emission of the membrane-potential-sensitive dye, diS-C_3-5, after mixing the cells with different concentrations of amphipathic-D. *C*, calcein release from the different cells, induced by amphipathic-D as a function of its concentration (*left panel*) and time (*right panel*). Calcein was entrapped into cells by incubation of 1 h. The cells were resuspended in PBS, and amphipathic-D was added to the cell suspensions. Peptide-induced calcein leakage resulted in an increase of fluorescence and was monitored at room temperature. The time-dependent curves include the peptide in its LC_{100} (50 μM, 80 μM, 300 μM, and 400 μM for CL1, 22RV1, OL, and 3T3 cells, respectively). The different cells are 3T3 fibroblasts (□), OL foreskin cells (○), 22RV1 prostate carcinoma cells (■), and CL1 prostate carcinoma cells (●). The results of four independent experiments were averaged with SD not exceeding 10%. *Bars*, ±SD.

neither indifference ($1.0 < FLC \leq 2.0$) nor antagonism ($FLC > 2.0$) was observed. Experiments were repeated three times with a SD of 5%.

Amphipathic-D but not Amphipathic-L Inhibits Prostate Tumor Growth in Xenografts and Lowers the PSA Level. CL1 and 22RV1 cells were implanted s.c. in mice, and the peptides were injected intratumorally at a dose of 1 mg/kg (stock solution of 0.1 mM), starting two weeks after tumor cell implantation. Dose response studies with 0.1 mg/kg, 0.5 mg/kg, 1 mg/kg, 3 mg/kg, and 5 mg/kg revealed 1 mg/kg as the optimal dose. A significant reduction in tumor weight was observed only with mice treated with amphipathic-D (see Figs. 3 and 4*A* for 22RV1; and Fig. 4*B* for CL1 xenografts). Most importantly, the tumor completely disappeared in 40% of the mice. A significant reduction in tumor weights was observed from day 13 until day 28, reaching 4-fold in the mean weight of both left tumors (Fig. 4, *A* and *B*). Furthermore, in the PSA-secreting 22RV1 xenografts (33), the reduction in tumor weight was accompanied by a marked lowering of the PSA serum levels (Fig. 4*C*). Note also that treatment with amphipathic-D resulted in an increase in the body weight of the animals compared with the vehicle-treated control group (data not shown). In contrast, amphipathic-L was inactive in both xenograft models. Moreover, the peptide caused sever necrosis on the skin of the animal in the area of injection (Fig. 3*A*, right panel).

Tumors contain extracellular matrix (ECM), therefore, we studied its interactions with the peptides. Briefly, amphipathic-D and amphipathic-L were mixed with Matrigel matrix for 1 h, and the solution was analyzed by using reverse phase-high-performance liquid chromatography and mass spectroscopy. The data revealed that amphipathic-L was fully inactivated by the Matrigel, in contrast to amphipathic-D, which preserved ~50% of its activity (data not shown).

Preliminary acute toxicity of the peptide was also examined by i.v. injecting mice ($n = 5$) with a single dose of a 0.9-ml solution containing 9 mg/kg/day for 5 days. No mortality and no long-lasting side effects were observed. All of the differential and biochemistry tests were in the range of normal values.

Histological Examination. Tumor sections taken 6 weeks after cell implantation revealed that amphipathic-D but not amphipathic-L inhibited the growth of prostate carcinoma cells. Fig. 3*C* shows the histological sections only for 22RV1 cells. The data revealed that in both the control xenografts (left panel) and those treated with amphipathic-L (right panel) most of the ECM was replaced by tumor cells. This is in contrast with mice treated with amphipathic-D, in which the number of tumor cells was reduced dramatically (middle panel).

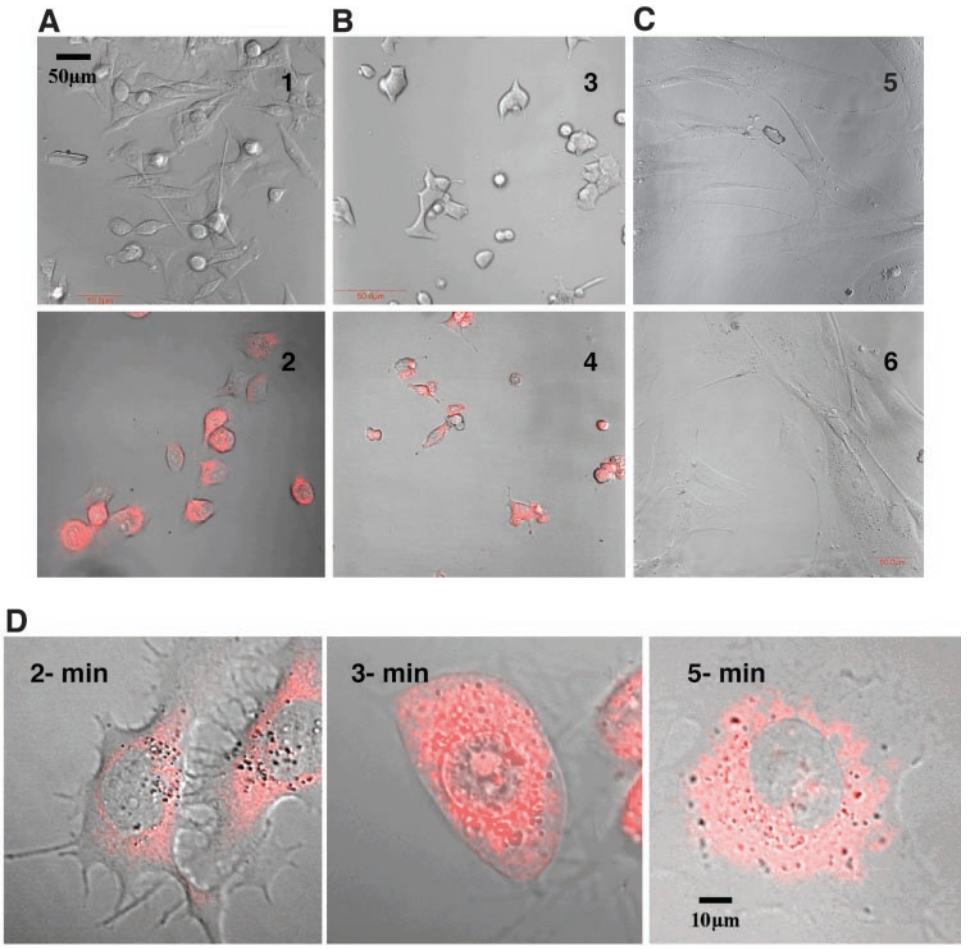

Fig. 2. Confocal laser scanning microscopy images of CL1 (*A*) and 22RV1 (*B*) prostate carcinoma cells and normal OL foreskin (*C*) cells untreated (*top panels*) and treated (*bottom panels*) with 5 μM rhodamine-labeled amphipathic-D. Cells were placed on a coverslip, and a series of images were taken before and 3 min after the addition of rhodamine-labeled peptide, using oil immersion. *D*, confocal laser scanning microscopy images of CL1 prostate carcinoma cells after 2-min, 3-min, and 5-min treatments with the rhodamine-labeled peptide (50 μM in PBS).

DISCUSSION

The most important result is that amphipathic-D but not its all L-amino acids parental peptide, amphipathic-L, markedly reduced tumor weights in both CL1 and 22RV1 prostate carcinoma xenografts, and the tumor completely disappeared in 40% of the mice. The histological evaluation showed necrotic debris in the sections taken from the remaining tumors treated with amphipathic-D, and the density of the cells was very low (Fig. 3*C*). This is in contrast with the significantly higher amount of mitotic cells in the untreated tumor or tumors treated with amphipathic-L. These results demonstrate that the remaining tumor does not proliferate normally. Furthermore, the reduction in the tumor size was accompanied by a drastic lowering of the PSA level in the 22RV1 xenografts, which secrete this antigen (33). Note that amphipathic-L did not inhibit PSA synthesis, suggesting that the reduction in the PSA level was probably due to the reduction in tumor size. Therefore, prolonged treatment with amphipathic-D is not likely to interfere with the validity of PSA as an indicator of prostate carcinoma progression, in contrast to other drugs, such as antiandrogen or antiestrogen chemotherapeutics (42).

The finding that amphipathic-L is not active *in vivo*, despite being highly potent *in vitro*, can be explained partially by the fact that it loses activity in serum, and because it is inactivated by the ECM. In contrast, amphipathic-D preserves full activity in serum and ~50% of its activity in the presence of ECM. Any drug, when locally administered, first needs to traverse the preexisting ECM, which provides a complex combination of insoluble molecules, which together with soluble growth factors and intracellular contacts modulates cell function (43).

Interestingly, despite being similarly active on cancer cells (Table 1) and bacteria (44), amphipathic-D but not amphipathic-L is selective toward prostate carcinoma cells (Table 1; Fig. 1*A*, left panel). A plausible explanation for this selective activity could be as follows: A common feature found in amphipathic-L and all of the other noncell-selective peptides is their stable amphipathic α-helical structure in membranes as well as their similar affinity to negatively charged and zwitterionic membranes. Structural studies revealed that both amphipathic-L and amphipathic-D have unordered structures in solution (31). However, whereas amphipathic-L strongly binds and becomes fully helical in any type of membrane, amphipathic-D binds ~15-fold better negatively charged membranes compared with zwitterionic membranes (45). This binding is governed mainly by electrostatic interactions (45). Membrane binding forces the peptide to adopt a functional structure, which allows destabilization of the membrane (31). In agreement with this, many cancer cells have approximately

Table 2 *Checkerboard titrations of combinations of amphipathic-D with different chemotherapeutic agents*

Chemotherapeutic agent	Cell type	FLC index*	Effect
Doxorubicin	CL1 prostate carcinoma	0.44	Synergism
	22RV1 prostate carcinoma	0.49	Synergism
	LNCaP prostate carcinoma	0.49	Synergism
Cyclophosphamide	CL1 prostate carcinoma	0.57	Additivity
	22RV1 prostate carcinoma	0.66	Additivity
	LNCaP prostate carcinoma	0.63	Additivity

* FLC index = $FLC_A + FLC_B = [(A)/LC_{100A}] + [(B)/LC_{100B}]$, where LC_{100A} and LC_{100B} are the LC_{100}s of drugs A and B when used alone, and (A) and (B) are the LC_{100}s of drugs A and B when used in combination. Experiments were repeated three times with an SD of 5%.

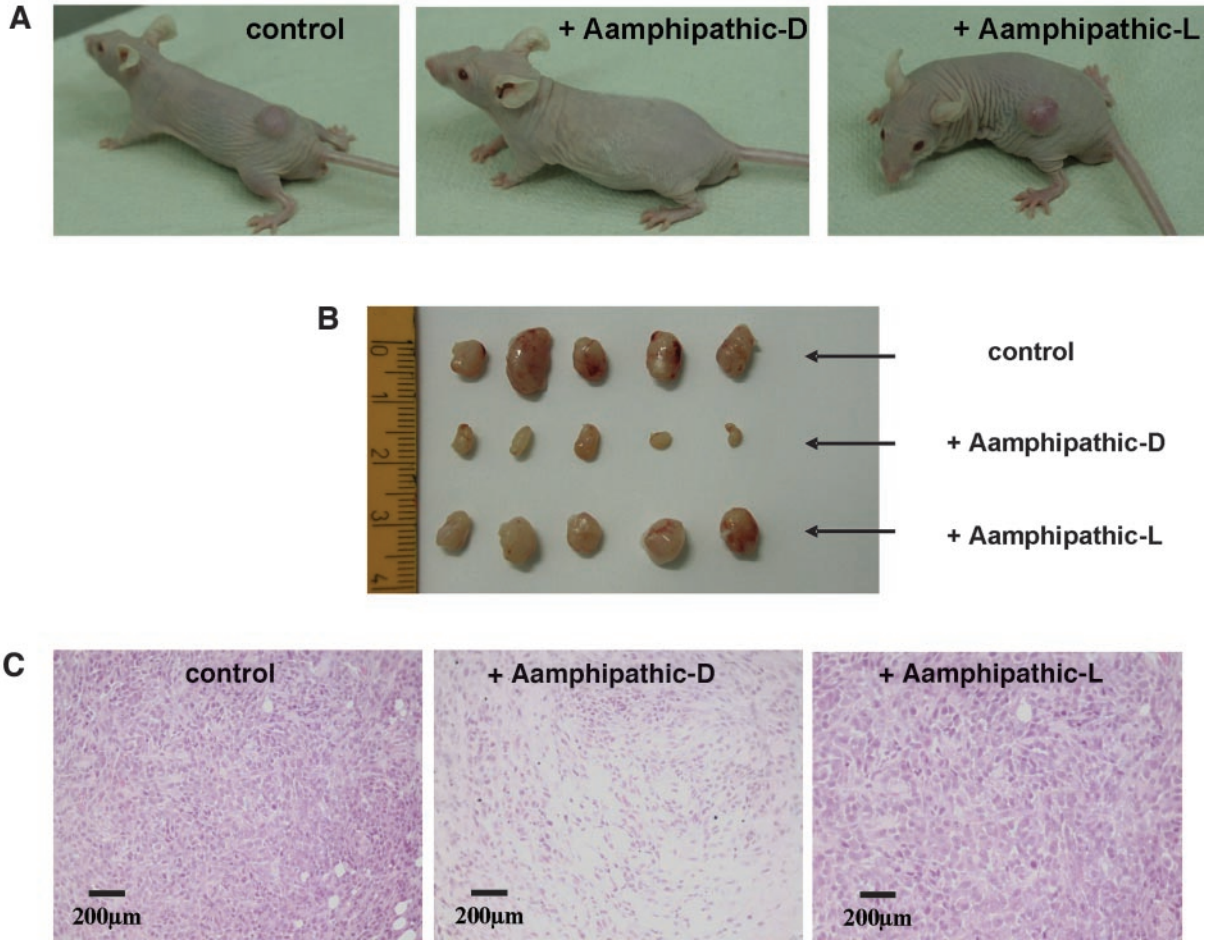

Fig. 3. Reduction in 22RV1 tumor weight in CD1 nude mice after intratumor administration of amphipathic-D and amphipathic-L. *A*, the dorsal side of mice injected with 22RV1 tumor cells and intratumorally treated with amphipathic-D (*middle panel*), amphipathic-L (*right panel*), or vehicle control (*left panel*). Note the necrotic skin area in the mice (*right panel*) after treatment with amphipathic-L. *B*, 22RV1 tumors of mice treated with amphipathic-D, amphipathic-L, or vehicle control. The peptides at 1 mg/kg (50 μl of 0.1 mM) were intratumorally administered to animals that were inoculated s.c. with human 22RV1 prostate carcinoma cells in Matrigel. *C*, histological evaluation of 22RV1 tumors after treatment with amphipathic-D (*middle panel*), amphipathic-L (*right panel*), or vehicle control (*left panel*). At 4 weeks, tumors were collected for histological examination. Serial 4-μm sections were prepared after the samples had been embedded in Paraplast. The sections were stained with hematoxylin and eosin.

2–4% more acidic phospholipids in their outer leaflet, and together with *O*-glycosylated mucines [high molecular weight glycoproteins consisting of a backbone protein to which oligosaccharides are attached via the hydroxylic groups of serine or threonine (46)] they create the additional negative charge. Nevertheless, we cannot rule out the possibility that the higher negative potential inside cancer cells, compared with noncancer cells, also contributes to the selective lytic activity of amphipathic-D.

Although a necrotic rather than an apoptotic mechanism of killing is suggested, the details by which amphipathic-D kills prostate carcinoma cells is still not fully understood. Among the hundreds of antimicrobial peptides isolated thus far, only a few were investigated for their mode of action on cancer cells (27).[3] Most of these studies included many biophysical techniques conducted mainly with model phospholipid membranes (29, 47). To better understand the killing mechanism, we used predominantly living cells and evaluated the data from killing curves, binding studies, fluorescent dye efflux, and membrane potential experiments. All of these experiments were conducted under identical experimental conditions. We observed a necrotic process that involves four major steps in the following order: (*a*) amphipathic-D binds initially to distinct sites on the cytoplasmic membrane of the cell, probably due to the nonhomogeneous distribution of anionic phospholipids or other acidic components in its outer leaflet (29, 48), and then it reaches a threshold concentration; (*b*) the peptide induces marked membrane depolarization; (*c*) the kinetics of membrane permeation is fast followed by an equal distribution of the peptide in the cytoplasm; and (*d*) the cells die. These steps are similar to those observed with the cytolytic perforin produced by killer lymphocytes, which kill its target cells by puncturing their membranes (49).

Finally, we show that amphipathic-D acts synergistically with doxorubicin toward all types of cells including androgen-independent and androgen-dependent, and, therefore, the status of hormone-dependency does not seem to affect this synergism. This is in contrast to other chemotherapeutics, such as the proapoptotic tumor necrosis factor-related apoptosis-inducing ligand that acts synergistically with the proteasome inhibitor bortezomib on LNCaP prostate carcinoma but has an antagonistic effect on CL1 prostate carcinoma. The mechanism of the synergism by amphipathic-D still remains largely unknown. Nevertheless, one possibility is its ability to increase the permeability of the cell to other chemotherapeutics.

In summary, this study shows that amphipathic-D, but not its parental amphipathic-L peptide, can be administered intratumorally, and it dramatically reduces the tumor growth of various human prostate carcinoma xenografts. Note, however, that membrane-active peptides are known to be toxic when injected i.v. at high doses. Here,

[3] See a partial list at http://aps.unmc.edu/AP/main.html.

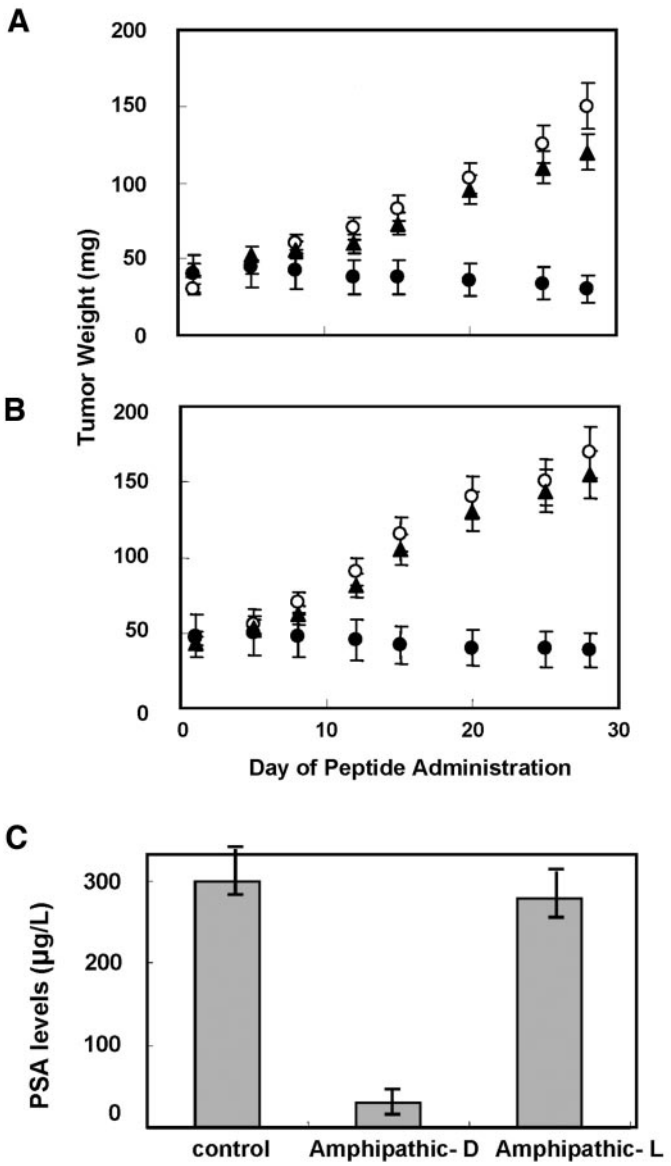

Fig. 4. Reduction in 22RV1 (*A*) and CL1 (*B*) tumor weight in CD1 nude mice after intratumor administration of amphipathic-D and amphipathic-L. Tumor growth curve of postadministration of amphipathic-D (●), amphipathic-L (▲), or vehicle control (○). $P < 0.005$, Student's *t* test. *C*, prostate-specific antigen (*PSA*) serum levels in mice injected with 22RV1 PC cells and then treated with amphipathic-D, amphipathic-L, or vehicle control. Amphipathic-D and amphipathic-L, at 1 mg/kg (50 μl of 0.1 mM), were intratumorally administered to animals that were inoculated s.c. with human 22RV1 or CL1 prostate carcinoma cells in Matrigel. Tumor weight (mg) was monitored and recorded twice a week during the period of 28 days. At 4 weeks, blood was withdrawn from the mice for PSA determination. The results of three independent experiments were averaged with SD not exceeding 10%. *Bars*, ±SD.

i.v. injection of amphipathic-D at a dose of 9-fold higher than the intratumor dose was not detrimental to the mice (data not shown). In addition, we have shown recently that a diastereomeric peptide significantly inhibited lung metastasis formation in mice when injected i.v. (31). Note also that although peptides can be weakly immunogenic, several reports indicate that free, short antimicrobial peptides do not induce an antibody response when injected into mice. In addition, the immunogenicity of short fragments containing D- L-amino acids has been shown to be reduced markedly compared with their all-L- or all-D-amino acid parent molecules (50). The unique properties of the diastereomer and its strong membranolitic effect should make it difficult for the tumor cell to develop resistance. Furthermore, amphipathic-D, together with other chemotherapeutic agents, represents a promising drug combination that should be explored additionally for therapeutic use.

ACKNOWLEDGMENTS

We thank Arik Makovitzki and Tova Waks for their help in the *in vivo* experiments. We are also grateful to Menachem Rubinstein for providing us human OL foreskin fibroblasts, Dr. Alon Harmelin for his assistance in the histologic evaluation, and Vladimir Kiss for his technical support in the confocal microscopy studies.

REFERENCES

1. Coffey DS. Prostate cancer. An overview of an increasing dilemma. Cancer (Phila) 1993;71:880–6.
2. Wingo PA, Tong T, Bolden S. Cancer statistics, 1995. CA - Cancer J Clin 1995;45: 8–30.
3. Landis SH, Murray T, Bolden S, Wingo PA. Cancer statistics, 1998. CA - Cancer J Clin 1998;48:6–29.
4. Obasaju C, Hudes GR. Paclitaxel and docetaxel in prostate cancer. Hematol Oncol Clin North Am 2001;15:525–45.
5. Thomas T, Balabhadrapathruni S, Gallo MA, Thomas TJ. Development of polyamine analogs as cancer therapeutic agents. Oncol Res 2002;13:123–35.
6. Morrissey C, Watson RW. Phytoestrogens and prostate cancer. Curr Drug Targets 2003;4:231–41.
7. Petrylak DP. Chemotherapy for advanced hormone refractory prostate cancer. Urology 1999;54:30–5.
8. Beer T, Raghavan D. Chemotherapy for hormone-refractory prostate cancer: beauty is in the eye of the beholder. Prostate 2000;45:184–93.
9. van Brussel JP, Busstra MB, Lang MS, et al. A phase II study of temozolomide in hormone-refractory prostate cancer. Cancer Chemother Pharmacol 2000;45:509–12.
10. Howell SB. Resistance to apoptosis in prostate cancer cells. Mol Urol 2000;4:225–9.
11. Gjertsen BT, Logothetis CJ, McDonnell TJ. Molecular regulation of cell death and therapeutic strategies for cell death induction in prostate carcinoma. Cancer Metastasis Rev 1998;17:345–51.
12. Munshi A, McDonnell TJ, Meyn RE. Chemotherapeutic agents enhance TRAIL-induced apoptosis in prostate cancer cells. Cancer Chemother Pharmacol 2002;50: 46–52.
13. Modur V, Nagarajan R, Evers BM, Milbrandt J. FOXO proteins regulate tumor necrosis factor-related apoptosis inducing ligand expression. Implications for PTEN mutation in prostate cancer. J Biol Chem 2002;277:47928–37.
14. Baker MA, Maloy WL, Zasloff M, Jacob LS. Anticancer efficacy of Magainin2 and analogue peptides. Cancer Res 1993;53:3052–7.
15. Ellerby HM, Arap W, Ellerby LM, et al. Anti-cancer activity of targeted pro-apoptotic peptides. Nat Med 1999;5:1032–8.
16. Chen Y, Xu X, Hong S, et al. RGD-Tachyplesin inhibits tumor growth. Cancer Res 2001;61:2434–8.
17. Mai JC, Mi Z, Kim SH, Ng B, Robbins PD. A proapoptotic peptide for the treatment of solid tumors. Cancer Res 2001;61:7709–12.
18. Boman HG. Peptide antibiotics and their role in innate immunity. Annu Rev Immunol 1995;13:61–92.
19. Biragyn A, Surenhu M, Yang D, et al. Mediators of innate immunity that target immature, but not mature, dendritic cells induce antitumor immunity when genetically fused with nonimmunogenic tumor antigens. J Immunol 2001;167:6644–53.
20. Yang D, Biragyn A, Kwak LW, Oppenheim JJ. Mammalian defensins in immunity: more than just microbicidal. Trends Immunol 2002;23:291–6.
21. Oppenheim JJ, Biragyn A, Kwak LW, Yang D. Roles of antimicrobial peptides such as defensins in innate and adaptive immunity. Ann Rheum Dis 2003;62:ii17–21.
22. Hui L, Leung K, Chen HM. The combined effects of antibacterial peptide cecropin A and anti-cancer agents on leukemia cells. Anticancer Res 2002;22:2811–6.
23. Shin SY, Lee SH, Yang ST, et al. Antibacterial, antitumor and hemolytic activities of alpha-helical antibiotic peptide, P18 and its analogs. J Pept Res 2001;58:504–14.
24. Park Y, Lee DG, Jang SH, et al. A Leu-Lys-rich antimicrobial peptide: activity and mechanism. Biochim Biophys Acta 2003;21:172–82.
25. Warren P, Li L, Song W, et al. In vitro targeted killing of prostate tumor cells by a synthetic amoebapore helix 3 peptide modified with two gamma-linked glutamate residues at the COOH terminus. Cancer Res 2001;61:6783–7.
26. Leuschner C, Enright FM, Gawronska B, Hansel W. Membrane disrupting lytic peptide conjugates destroy hormone dependent and independent breast cancer cells in vitro and in vivo. Breast Cancer Res Treat 2003;78:17–27.
27. Wang Z, Wang G. APD: the antimicrobial peptide database. Nucleic Acids Res 2004;32:D590–2.
28. Chan SC, Yau WL, Wang W, et al. Microscopic observations of the different morphological changes caused by anti-bacterial peptides on Klebsiella pneumoniae and HL-60 leukemia cells. J Pept Sci 1998;4:413–25.
29. Papo N, Shai Y. New lytic peptides based on the D, L amphipathic helix motif preferentially kill tumor cells compared with nornal cells. Biochemistry 2003;42: 9346–54.
30. Oren Z, Shai Y. Selective lysis of bacteria but not mammalian cells by diastereomers of melittin: Structure-function study. Biochemistry 1996;36:1826–35.

31. Papo N, Shahar M, Eisenbach L, Shai Y. A novel lytic peptide composed of D, L amino acids selectively kills cancer cells in culture and in mice. J Biol Chem 2003;278:21018–23.
32. Patel BJ, Pantuck AJ, Zisman A, et al. CL1-GFP: an androgen independent metastatic tumor model for prostate cancer. J Urol 2000;164:1420–5.
33. Sramkoski RM, Pretlow TG II, Giaconia JM, et al. A new human prostate carcinoma cell line, 22Rv1. In Vitro Cell Dev Biol Anim 1999;35:403–9.
34. Horoszewicz JS, Leong SS, Chu TM, et al. The LNCaP cell line–a new model for studies on human prostatic carcinoma. Prog Clin Biol Res 1980;37:115–32.
35. Merrifield RB, Vizioli LD, Boman HG. Synthesis of the antibacterial peptide cecropin A (1–33). Biochemistry 1982;21:5020–31.
36. Pouny Y, Shai Y. Interaction of D-amino acid incorporated analogues of pardaxin with membranes. Biochemistry 1992;31:9482–90.
37. Allen TM, Cleland LG. Serum-induced leakage of liposome contents. Biochim Biophys Acta 1980;597:418–26.
38. Cercenado E, Eliopoulos GM, Wennersten CB, Moellering RC Jr. Absence of synergistic activity between ampicillin and vancomycin against highly vancomycin-resistant enterococci. Antimicrob Agents Chemother 1992;36:2201–3.
39. Gavish Z, Pinthus JH, Barak V, et al. Growth inhibition of prostate cancer xenografts by halofuginone. Prostate 2002;51:73–83.
40. Habermann E, Jentsch J. Hoppe Seyler's Z. Physiol Chem 1967;348:37–50.
41. Johansson J, Gudmundsson GH, Rottenberg ME, Berndt KD, Agerberth B. Conformation-dependent antibacterial activity of the naturally occurring human peptide LL-37. J Biol Chem 1998;273:3718–24.
42. Kelloff GJ, Lieberman R, Steele VE, et al. Agents, biomarkers, and cohorts for chemopreventive agent development in prostate cancer. Urology 2001;57:46–51.
43. Lukashev ME, Werb Z. ECM signalling: orchestrating cell behaviour and misbehaviour. Trends Cell Biol 1998;8:437–41.
44. Papo N, Oren Z, Pag U, Sahl HG, Shai Y. The consequence of sequence alteration of an amphipathic alpha-helical antimicrobial peptide and its diastereomers. J Biol Chem 2002;277:33913–21.
45. Papo N, Shai Y. Effect of drastic sequence alteration and d-amino acid incorporation on the membrane binding behavior of lytic peptides. Biochemistry 2004;43:6393–403.
46. Cappelli G, Paladini S, D'Agata A. Tumor markers in the diagnosis of pancreatic cancer. Tumori 1999;85:S19–21.
47. Chen HM, Wang W, Smith D, Chan SC. Effects of the anti-bacterial peptide cecropin B and its analogs, cecropins B-1 and B-2, on liposomes, bacteria, and cancer cells. Biochim Biophys Acta 1997;1336:171–9.
48. Hendrich AB, Michalak K. Lipids as a target for drugs modulating multidrug resistance of cancer cells. Curr Drug Targets 2003;4:23–30.
49. Liu CC, Walsh CM, Young JD. Perforin: structure and function. Immunol Today 1995;16:194–201.
50. Benkirane N, Friede M, Guichard G, et al. Antigenicity and immunogenicity of modified synthetic peptides containing D-amino acid residues. Antibodies to a D-enantiomer do recognize the parent L-hexapeptide and reciprocally. J Biol Chem 1993;268:26279–85.
51. An J, Sun YP, Adams J, et al. Drug interactions between the proteasome inhibitor bortezomib and cytotoxic chemotherapy, tumor necrosis factor (TNF) alpha, and TNF-related apoptosis-inducing ligand in prostate cancer. Clin Cancer Res 2003;9:4537–45.

Suppression of Human Prostate Tumor Growth in Mice by a Cytolytic d-, l-Amino Acid Peptide: Membrane Lysis, Increased Necrosis, and Inhibition of Prostate-Specific Antigen Secretion

Niv Papo, Amir Braunstein, Zelig Eshhar, et al.

Cancer Res 2004;64:5779-5786.